Contents lists available at ScienceDirect

EBioMedicine

Research paper

Pharmacological blockade of PCAF ameliorates osteoarthritis development via dual inhibition of TNF-α-driven inflammation and ER stress

Deheng Chen [a,b,1], Di Lu [a,b,1], Haixiao Liu [a,b], Enxing Xue [a,b], Yu Zhang [a,b], Ping Shang [c,*], Xiaoyun Pan [a,b,**]

[a] Department of Orthopaedics, The Second Affiliated Hospital and Yuying Children's Hospital of Wenzhou Medical University, 109, Xueyuanxi road, Wenzhou, Zhejiang 325027, China
[b] Bone Research Institute, The Key Orthopaedic Laboratory of Zhejiang Province, 109, Xueyuanxi road, Wenzhou, Zhejiang 325027, China
[c] Department of Rehabilitation, The Second Affiliated Hospital and Yuying Children's Hospital of Wenzhou Medical University, 109, Xueyuanxi road, Wenzhou, Zhejiang 325027, China

ARTICLE INFO

ABSTRACT

Background: Epigenetic mechanisms have been reported to play key roles in osteoarthritis (OA) development. P300/CBP-associated factor (PCAF) is a member of the histone acetyltransferases, which exhibits a strong relationship with endoplasmic reticulum (ER) stress and transcription factor nuclear factor kappa B (NF-κB) signals. Salidroside, a natural histone acetylation inhibitor, showed its anti-inflammatory and anti-apoptotic effects in lipopolysaccharide (LPS)-stimulated microglia cells in our previous study. However, whether Sal has a protective effect against OA remains unknown, and its relationships to PCAF, NF-κB, and the ER stress pathway should be explored further.
Methods: We identified the role of PCAF in the pathogenesis of OA and determined the chondroprotective effect of Sal on both tumor necrosis factor alpha (TNF-α)-treated human chondrocytes and a destabilized medial meniscus (DMM) mouse OA model.
Findings: We found increased PCAF expression in human OA cartilage and TNF-α-driven chondrocytes. Meanwhile, silencing of PCAF attenuated nuclear p65 and C/EBP homologous protein levels in chondrocytes upon TNF-α stimulation. Furthermore, Sal was found to specifically bind to the inhibitory site of the PCAF protein structure, which subsequently reversed the TNF-α-induced activation of NF-κB signal and ER stress-related apoptosis in chondrocytes. In addition, the protective effect of Sal and its inhibitory effects on PCAF as well as inflammatory- and ER stress-related markers were also observed in the mouse DMM model.
Interpretation: Pharmacological blockade of PCAF by Sal ameliorates OA development via inhibition of inflammation and ER stress, which makes Sal a promising therapeutic agents for the treatment of OA.

1. Introduction

With the combined effects of ageing and increasing obesity in the global population, the number of patients with degenerative osteoarthritis (OA) has reached 250 million; thus, OA may lead to significant socioeconomic problems. OA is a general degenerative disease, and the main symptoms are pain and joint disability among the elderly [1,2]. It is characterized by progressive injury of articular cartilage, subchondral bone remodeling, and synovitis [1]. Previous studies indicated that various factors contribute to the development of OA, including aging, obesity, trauma, and congenital anomalies [1,3]. Although the exact pathogenesis of OA remains unknown, it is widely acknowledged that inflammatory cytokines, especially tumor necrosis factor alpha (TNF-α), act as mediators that trigger an imbalance between anabolism and catabolism of articular cartilage [4,5]. This devastative effect—driven by TNF-α—was reported to be associated with the activation of

* Corresponding author.
** Corresponding author at: Department of Orthopaedics, The Second Affiliated Hospital and Yuying Children's Hospital of Wenzhou Medical University, 109, Xueyuanxi road, Wenzhou, Zhejiang 325027, China.
E-mail addresses: 260809686@qq.com (P. Shang), Xiaoyunpan@126.com (X. Pan).
[1] These authors contributed equally to this work.

Research in context

Evidence before this study

Histone acetylation balance was reported to play a role in the pathology of OA. P300/CBP-associated factor (PCAF) is a member of the histone acetyltransferases, which exhibits a strong relationship with ER stress and NF-κB signals. However, the relationship between FCAF and OA remains unknown. Salidroside (Sal) as a novel natural compound was found to has anti-inflammatory and anti-apoptotic effects in neurodegenerative diseases according to our previous study. However, the role of Sal in joint degenerative disease such as OA and the underlying mechanism have not been examined.

Added value of this study

PCAF expression was found upregulated in human OA cartilage and TNF-α-driven chondrocytes. Meanwhile, silencing of PCAF by siRNA inhibited the activation of ER stress and NF-κB signals in human chondrocytes. Furthermore, Pharmacological blockade of PCAF by Sal also attenuated NF-κB related inflammatory response and ER stress-related apoptosis in chondrocytes under TNF-α and ameliorated mouse OA develepment.

Implications of all the available evidence

PCAF might participate in the pathology of OA. Sal is a promising therapeutic agent for the treatment of OA.

inflammatory cascades and aberrant endoplasmic reticulum (ER) stress [6,7]. Moreover, several studies have reported that TNF-α levels are elevated in the synovial fluid, cartilage, and synovium of OA patients [8–10].

The inflammatory response stimulated by TNF-α in chondrocytes is closely associated with the nuclear factor kappa B (NF-κB) signaling pathway [6,11]. Once stimulated by TNF-α, p65 binds to its specific DNA sequences to initiate a series of inflammatory or catabolic effects [12]. In addition, ER stress, characterized by misfolded and unfolded protein aggregates in the lumen of the ER, is a type of defense mechanism in the cell [13,14]. However, exposure to a chronic inflammatory environment would induce aberrant ER stress, which consequently leads to the excessive apoptosis of chondrocytes [7,15].

Histone acetylation balance, which is achieved by the regulation of acetyltransferases and deacetylases, was reported to play a role in the pathology of OA [16,17]. Although various histone deacetylases (HDACs), including members of the classical family and SIR2 family, are widely studied as protective factors in OA, studies focusing on acetyltransferases are relatively rare [18]. Nevertheless, p300/CBP-associated factor (PCAF), a member of the histone acetyltransferases (HATs), has been implicated in inflammatory, apoptotic, and metabolic pathways [19–21]. It was reported that PCAF specifically acetylates the Lys-122 residue of NF-κB, thereby affecting related inflammatory and catabolic gene expression [22]. A previous study also demonstrated that PCAF works as a coactivator of activating transcription factor 4 and is involved in the regulation of C/EBP homologous protein (CHOP) transcription in ER stress mediated by amino-acid starvation [23]. Hence, PCAF exhibits a strong relationship with NF-κB and ER stress signals and targeting it might be a promising therapeutic strategy for OA.

Few small-molecule inhibitors of HATs, especially PCAF, are currently serviceable. A well-recognized class of inhibitors targeting PCAF is the isothiazolones, which are potent but highly toxic to cells [24,25]. Also, their reactivity limits their specificity. Interestingly, it has been demonstrated that salidroside (Sal), a phenylpropanoid glycoside extracted from the root of *Rhodiola rosea*, has an inhibitory effect on histone acetylation [26]. Meanwhile, our previous study showed that the potential anti-inflammatory and anti-apoptotic effects of Sal were associated with the suppression of NF-κB and ER stress signals in lipopolysaccharide (LPS)-stimulated microglia cells [27]. However, whether Sal has a protective effect against OA remains unknown, and its relationships to PCAF, NF-κB, and the ER stress pathway should be explored further.

In our study, we investigated the expression levels of PCAF in human degenerative and normal cartilage. We also investigated the potential functional role of PCAF in OA pathology and the underlying molecular mechanisms. In addition, we determined the inhibitory potency of Sal on PCAF, examined its chondro-protective effect, investigated its exact mechanism in TNF-α-stimulated human chondrocytes, and applied it in a surgically-induced OA mouse model.

2. Materials and methods

2.1. Ethics statement

The experimental protocols, animal use, and postoperative animal care procedures were performed in accordance with the guidelines and principles of the Animal Care and Use Committee of Wenzhou Medical University, Wenzhou, China (ethics code: wydw2014-0129).

2.2. Reagents and antibodies

The following reagents and antibodies were used in this study: salidroside (C$_{14}$H$_{20}$O$_7$, CAS#:10338–51–9, Nanjing, China); recombinant human TNF-α, type II collagenase, and Safranin-O/Fast Green (Sigma-Aldrich, St. Louis, MO, USA).primary antibody against p65(Cat# 59674, RRID:AB_2799570), COX-2(Cat# 12282, RRID:AB_2571729), IκBα(Cat# 4812, RRID:AB_10694416), and XBP-1s (Cat# 12782, RRID:AB_2687943) were purchased from Cell Signaling Technology(Danvers, MA, USA); anti-iNOS (Cat# SAB4502012, RRID:AB_10744871) were bought from Sigma-Aldrich; antibodies against PCAF(Cat# ab110421, RRID:AB_11156343), H3K9ac(Cat# ab4441, RRID:AB_2118292), lamin-B1(Cat# ab22137, RRID:AB_446813), GAPDH(Cat# ab9485, RRID:AB_307275), cleaved caspase 3(Cat# ab2302, RRID:AB_302962), cleaved caspase 12(Cat# ab62484, RRID:AB_955729), cytochrome C(Cat# ab133504, RRID:AB_2802115), and cleaved PARP (Cat# ab32064, RRID:AB_777102) were obtained from Abcam (Cambridge, UK). Alexa Fluor 594- and Alexa Fluor 488-labelled anti-rabbit goat immunoglobulin G (H + L) inferior antibody were bought from Jackson Immuno Research (West Grove, PA, USA). Gibco (Carlsbad, CA, USA) provided cell-culture reagents.

2.3. Cell culture

Six OA patients provided human OA cartilage samples during surgery for total knee replacement (53–71 years old; Kellgren–Lawrence grade IV; $n = 6$) (representative X-ray data are presented in Supplementary Fig. S1). Control human articular cartilages from six donors with no significant clinical or imaging features of OA were obtained from femoral condyles at autopsy (44–68 years old; Kellgren–Lawrence grade 0; $n = 6$). For primary human chondrocyte culture, the cartilage was sliced into 1-mm^3 cubes and washed thrice with phosphate buffered saline (PBS).

Subsequently, the cartilage samples were lysed with 0.25% trypsin-ethylenediaminetetraacetic acid (EDTA) followed by 0.2% collagenase II in Dulbecco's modified Eagle medium/nutrient mixture F12 (DMEM/F12) at 37 °C for 6 h. After washing with PBS and centrifugation, the internal cellular mass was placed in DMEM/F12 with 12% fetal bovine serum. Plates were inoculated at 4×10^5 cells/ml, and the cells were cultivated in a moistened environment at 37 °C and 5% CO_2 followed by regular replacement of the medium every other day. To prevent phenotypic feature loss, passage 1–2 chondrocytes were used in western blot and immunofluorescence studies, and passage 2–3 chondrocytes were used in the rest studies. The entire study was approved by the medical ethics committee of the Second Affiliated Hospital of Wenzhou Medical University (number: LCKY-2017-36) and was performed in accordance with the guidelines of the Declaration of Helsinki [28]. Ethics approval is provided in Supplementary File 1. Informed consent was obtained from all participants.

2.4. siRNA transfection

Short interfering RNA (siRNA) against the human PCAF gene was designed and synthesized with the following sequence: 5′-AAUCGCCGUGAAGAAAGCGCA-3′ (RiboBio, Guangzhou, China). We seeded chondrocytes in six-well plates and cultured them to 60–70% confluence. Cells were then transfected with 50 nM siRNA or negative control with Lipofectamine 2000 for 36 h (Thermo Fisher, Logan, UT, USA) according to the manufacturer's instructions.

2.5. Molecular docking

We chose PCAF (PDB ID: 4NSQ) for docking studies [19]. The protein structure was prepared for docking analysis after it was downloaded from the Protein Data Bank (https://www.rcsb.org/). PyMoL (version 1.7.6; https://pymol.org) produced the least energy conformations with default limits. The analysis of protein–ligand docking with ligand binding flexibility and binding pocket residues was done using AutoDockTools (version 1.5.6; http://autodock.scripps.edu/resources/adt). Finally, images were generated from PyMoL files using UCSF Chimera (https://www.cgl.ucsf.edu/chimera).

2.6. Cell viability

Cell viability was assayed using the Cell Counting Kit-8 (CCK-8; Dojindo, Kumamoto, Japan) following the manufacturer's guidelines. In brief, human OA chondrocytes were cultivated in 96-well plates for 24 h and then pretreated with 0, 1, 5, 10, 40, or 100 μM Sal with or without stimulation by TNF-α (20 ng/ml) for 24 h. Thereafter, 100 μl of 10% CCK-8 solution was added to each plate, and the plates were incubated at 37 °C for 120 min. A microplate reader (Leica Microsystems, Wetzlar, Germany) was used to evaluate the absorbance of the wells at 450 nm. All experiments were performed six times.

2.7. Protein extraction

RIPA lysis buffer was used to isolate whole-cell proteins. Cytoplasmic and nuclear proteins were isolated using a Cytoplasmic and Nuclear Protein Extraction kit (Beyotime, Shanghai, China). The lysates were fragmented using ultra-wave sonication in an ice bath, followed by centrifugation at 4 °C and 12,000 rpm for 30 min. Histone extraction was performed as described previously. Briefly, the cell sample was lysed in hypotonic lysis buffer (10 mM Tris-HCl, 1.5 mM $MgCl_2$, 1 mM KCl, 1 mM phenylmethylsulfonyl fluoride, and 1.3 mM dithiothreitol; pH 8.0) with 10% NP-40. Nuclei were precipitated and subsequently incubated with 0.2 M H_2SO4 at 4 °C for 120 min. After centrifugation at 4 °C and 16,000 rpm, 100%

trichloroacetic acid was added to the precipitated histones, which were then washed twice with ice-cold acetone. Protein concentrations were measured using a BCA protein assay kit (Beyotime).

2.8. Western blot analysis

Sodium dodecyl sulfate polyacrylamide gel electrophoresis was used to separate equal amounts of protein (40 μg). This was followed by protein transfer to polyvinylidene difluoride membranes. After blocking with 5% nonfat milk for 2 h, the membranes were treated with primary antibodies against PCAF (1:500), H3K9ac (1:500), lamin B (1:5000), p65 (1:1000), CHOP (1:1000), GAPDH (1:5000), COX-2 (1:500), iNOS (1:1000), IkBα (1:1000), cleaved PARP (1:1000), cleaved caspase 3 (1:500), XBP-1s (1:1000), cleaved caspase 12 (1:1000), and cytochrome C (1:5000) overnight at 4 °C. The next day, the membranes were treated with the corresponding secondary antibodies (1:3000) for 2 h. The bands were detected via enhanced chemiluminescence (ECL) plus reagent (Invitrogen, Carlsbad, CA, USA). Finally, the bands detected via ECL were analyzed using Quantity ONE software (Bio-Rad Laboratories, Hercules, CA, USA). The standard proteins were lamin B and GAPDH.

2.9. Analysis of nitric oxide (NO), prostaglandin E2 (PGE2), interleukin (IL)-6, collagen II, aggrecan, matrix metalloproteinase 13 (MMP13), and ADAMTS-5 levels

The Griess reaction was used to determine NO levels in the culture medium, as described previously [29]. Briefly, a 100-μl suspension was treated with an equal volume of Griess reagent. After 10 min, a microplate reader was used to measure the absorbance at 540 nm. Fresh culture medium was used as a blank control. For quantification of PGE2, IL-6, collagen II, MMP13, ADAMTS-5, and aggrecan levels, 100 μl of culture medium supernatant was collected from each sample, and the concentrations of the secreted proteins were measured using enzyme-linked immunosorbent assay (ELISA) kits (R&D Systems, Minneapolis, MN, USA) according to the manufacturer's instructions.

2.10. Immunofluorescence

The chondrocytes were plated on crystal six-well plates and treated with 20 ng/ml TNF-α alone or co-treated with 20 ng/ml TNF-α and 40 μM Sal for 24 h (or for 2 h for p65). Next, the samples were fixed with 4% paraformaldehyde for 30 min, then permeabilized with 0.5% Triton X-100 in PBS for 15 min. Subsequently, the cells were blocked with 5% goat serum for 1 h, then treated with primary antibodies against MMP13 (1:200), p65 (1:200), and collagen II (1:200) at 4 °C overnight. The next day, Alexa Fluor 594-labeled or Alexa Fluor 488-conjugated secondary antibodies (1:400) were used for incubation at room temperature (RT) for 60 min, followed by DAPI labeling for 1 min. The images were captured and analyzed using fluorescence microscopy (Olympus, Tokyo, Japan).

Human and mouse cartilage tissues were fixed in 4% (v/v) neutral paraformaldehyde for 24 h, followed by a 1-month decalcification with neutral 10% (v/v) EDTA. After dehydration and embedding in paraffin, the tissues were sectioned with a thickness of 5 μm. The paraffin was removed from the sagittal sections using xylene, then the sections were moistened by numerous washes in ethanol for immunofluorescence staining. Sections were treated with 10% bovine serum albumin (BSA) for 1 h in PBS with 0.1% Triton X-100 (PBST). Sections were then incubated with the anti-PCAF (1:100) primary antibodies overnight at 4 °C in PBST. Next, sections were washed in PBST four times for 10 min, then incubated with Alexa Fluor 488-labeled goat anti-rabbit secondary antibody at RT for 1 h. Sections were incubated with pure DAPI for 10 min

and covered with cover slips. Five fields of each slide (six slides in each group) were randomly selected and analyzed under a fluorescence microscope by an examiner who was unaware of the group allocations.

2.11. TUNEL staining

After chondrocytes or cartilage sections were fixed, TUNEL staining was carried out using an In Situ Cell Death Detection kit (Roche, Basel, Switzerland) according to the manufacturer's instructions in a dark, humidified room. Next, DAPI was used to stain the cell nuclei. Positive staining of DNA strand breaks in apoptotic cells was detected under a fluorescence microscope.

2.12. Transmission electron microscopy (TEM)

Human OA chondrocytes were infiltrated with 2.5% glutaraldehyde overnight. The next day, cells were fixed in 2% osmium tetroxide for 1 h, then treated with 2% uranyl acetate for 60 min. After dehydration with acetone, samples were embedded in araldite and sliced into semi-thin sections. Subsequently, toluidine blue was used to stain slices to locate cell positions, and TEM (Hitachi, Tokyo, Japan) was used for observation.

2.13. Mouse model of OA

Sixty 10-week-old C57BL/6 male wild-type mice were purchased from the Animal Center of the Chinese Academy of Sciences, Shanghai, China. OA was induced by conventional surgery (destabilization of the medial meniscus; DMM), as described previously [30]. Briefly, mice were intraperitoneally injected with 2% (w/v) pentobarbital (40 mg/kg), then an experienced surgeon incised the joint capsule of the right knee medial to the patellar tendon and transected the medial meniscotibial ligament using microsurgical techniques. The left knee joint was used as the sham group, which underwent an arthrotomy only. After surgery, the
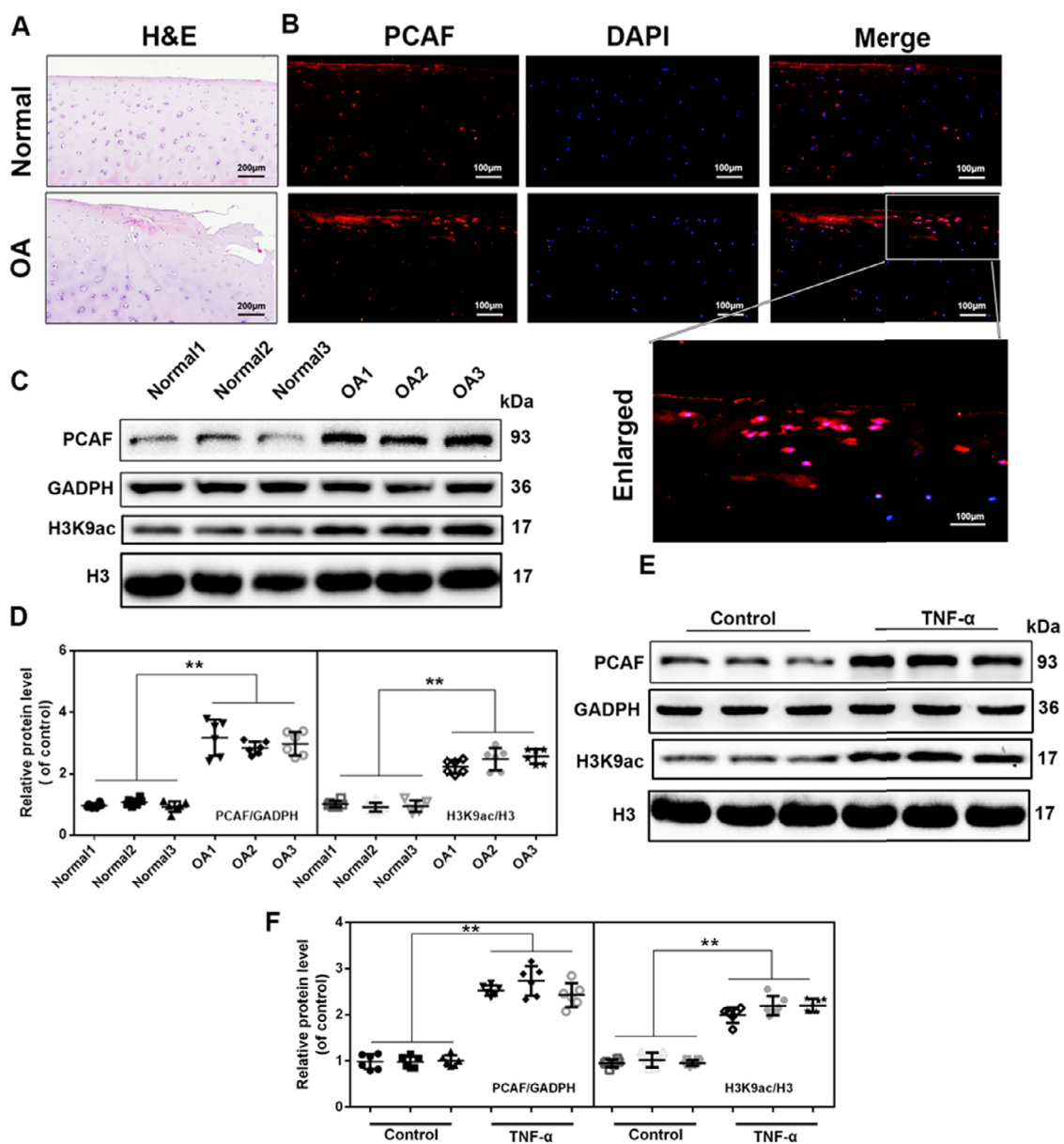

Fig. 1. Increased levels of PCAF in human OA cartilage and TNF-α-treated human chondrocytes. (A, B) Representative H&E staining and immunofluorescence staining of PCAF in cartilage tissues from normal and OA patients. (scale bar: 200 μm [A], 100 μm [B]). (C, D) PCAF and H3K9ac levels in chondrocytes derived from OA patients and controls. (E, F) PCAF and H3K9ac levels in human chondrocytes stimulated with 20 ng/ml TNF-α for 24 h. All results are presented as the means ± SDs of six duplicate experiments. *P < 0.05, **P < 0.01.

mice were randomly divided into three groups: the sham group, DMM group, and Sal treatment group. The salidroside group received the drug at 25 mg/kg/d everyday [31]. The sham group and DMM group received a volume of saline equal to that administered to the salidroside group. Animals were subjected to X-ray imaging of the knee joint at 8 weeks after knee surgery. The mice were then sacrificed, and knee joint specimens were gathered for the following experiments.

2.14. Histopathological analysis

Sections of human or mouse cartilage (5 μm thick) were stained with hematoxylin and eosin (H&E) or Safranin O/Fast Green (S-O) to evaluate cartilage degeneration. The histological assessment was performed blindly by experienced researchers according to the Osteoarthritis Research Society International (OARSI) scoring system [32]. The severity of synovitis was graded using a previously described scoring system [33]—synovial coating cell layer expansion was graded using a Likert scale of 0–3 (0: 1–2 cells; 1: 2–4 cells; 2: 4–9 cells; and 3: >10 cells), and synovial stroma cell compactness was graded using a Likert scale of 0–3 (0: typical cellularity; 1: slightly increased cellularity; 2: moderately enlarged cellularity; and 3: greatly enlarged cellularity).

2.15. Immunohistochemical analysis

Following dehydration and embedding in paraffin, the tissues were sectioned with a thickness of 5 μm. For immunohistochemical analysis, xylene was used for deparaffinization, and ethanol was used for rehydration. Subsequently, the sections were blocked with 3% hydrogen peroxide and then treated with 0.4% pepsin for 20 min in 5 mM HCl at 37 °C for antigen recovery. Next, the sections were incubated with 10% BSA for 30 min, followed by incubation with primary antibody (anti-collagen II, 1:200; anti-MMP13, 1:200) overnight at 4 °C. The next day, the sections were treated with the corresponding secondary antibodies (Santa Cruz

Biotechnology, Dallas, TX, USA) and counterstained with hematoxylin. Image-Pro Plus software (version 6.0; Media Cybernetics, Rockville, MD, USA) was used for analysis. Five fields of each slide (six slides in each group) were selected randomly and captured under a fluorescence microscope to count inducible NO synthase (iNOS)-positive cells.

2.16. Statistical analysis

The experiments were done for 6 biological replicates and 3 technical replicates. Outcomes are presented as the means ± standard deviations (SDs). Statistical analyses were performed using SPSS statistical software (version 20.0; IBM Corporation, Armonk, NY, USA). The variance of two or more groups was analyzed using one-way analysis of variance followed by Tukey's test. Nonparametric data were analyzed using the Kruskal–Wallis H test. A P-value < 0.05 indicated statistical significance.

3. Results

3.1. PCAF expression was up-regulated in human degenerative cartilage and TNF-α-stimulated chondrocytes

PCAF immunofluorescence staining and western blot analysis were performed to investigate the association between PCAF levels and OA in patients. Histology revealed that OA cartilage exhibited surface erosion and apparent hypocellularity (Fig. 1(A)). PCAF immunofluorescence revealed that there was a higher expression of PCAF in the cartilage from OA patients (Fig. 1(B)), and western blot analysis indicated that there were increased levels of PCAF and H3K9ac in the chondrocytes taken from OA subjects compared to those from the control group (Fig. 1(C) and (D)). Meanwhile, based on western blot analysis, we found that TNF-α induced higher expression of PCAF and acetylation on histone H3 lysine 9 (H3K9ac) in human chondrocytes (Fig. 1(E) and (F)).
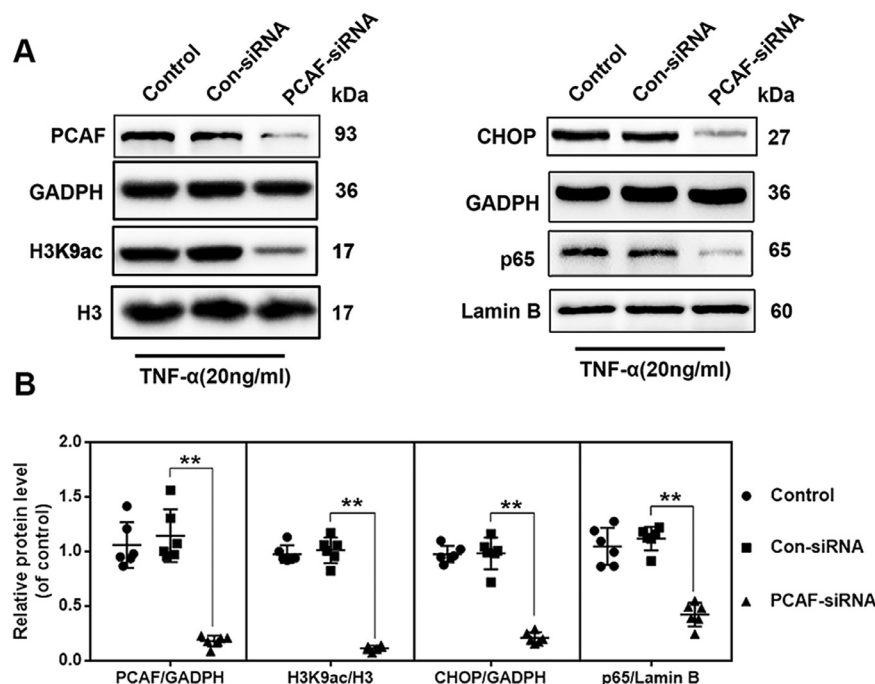

Fig. 2. Silencing PCAF attenuated nuclear p65 and CHOP levels under TNF-α stimulation. (A, B) The levels of PCAF, H3K9ac, p65, and CHOP in chondrocytes transfected with control siRNA and PCAF siRNA under TNF-α stimulation. All results are presented as the means ± SDs of six duplicate experiments. *P < 0.05, **P < 0.01.
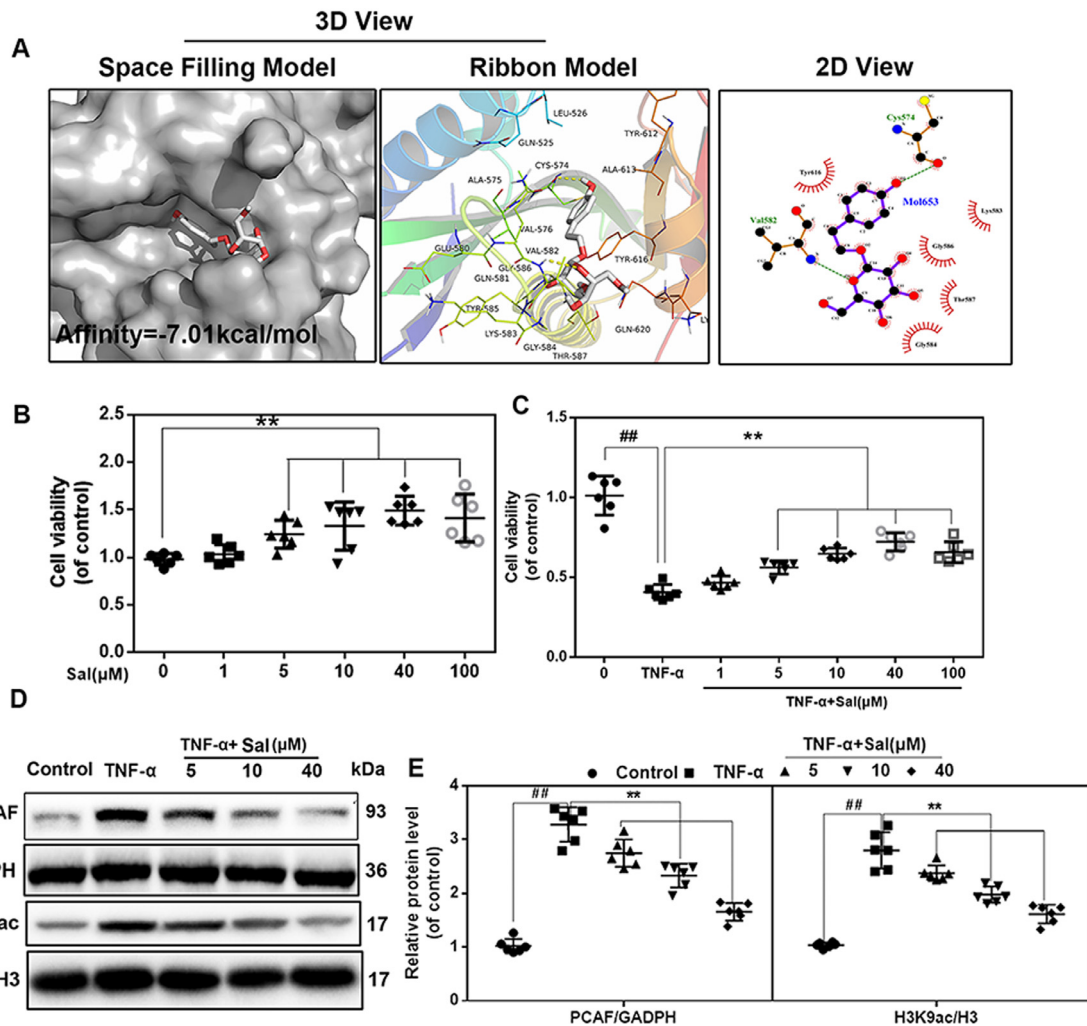
Fig. 3. Sal specifically inhibited PCAF expression. (A) Sal docked with the PCAF structure. Docking studies were performed as described in Section 2. The space-filling model shows the binding of Sal in the inhibitory binding pocket. The protein residues and hydrogen bonds are shown in a ribbon model. Hydrophobic bonds are shown in 2-D view. (B, C) The viability of human chondrocytes after Sal treatment at different concentrations with or without TNF-α stimulation. (D, E) PCAF and H3K9ac levels in human chondrocytes pretreated with Sal at different concentrations and stimulated with 20 ng/ml TNF-α. All results are presented as the means $\pm$ SDs of six duplicate experiments. $^{\#\#}P < 0.01$ compared to the control group; $^{*}P < 0.05$, $^{**}P < 0.01$ compared to the TNF-α alone group.

3.2. PCAF silencing inhibited TNF-α-induced activation of nuclear p65 and CHOP expression

PCAF silencing was performed using PCAF siRNA transfection, and western blotting confirmed that PCAF expression was markedly reduced. Compared to cells treated with control siRNA under TNF-α stimulation, PCAF siRNA decreased H3K9ac, nuclear p65, and CHOP levels (Fig. 2(A) and (B)).

3.3. Sal specifically inhibited PCAF expression in TNF-α-stimulated human chondrocytes

The crystal structure of PCAF in a complex with coenzyme A has been published previously [34]. Using this structure, docking studies were performed to propose a possible binding mode for Sal. We found that Sal formed several favorable connections and docked nicely within the inhibitory binding site of PCAF. Fig. 3(A) shows a space-filling model that directly illustrates the coverage of Sal in the protein structure of PCAF. As calculated using AutoDock-Tools, Sal has a high affinity of −7.01 kcal/mol for PCAF. Meanwhile, local interactions of protein residues were visualized using a ribbon model. Important hydrogen bonds were formed between Sal and Val582 and Cys574 of PCAF. Furthermore, the 2-D

view shows that several hydrophobic bonds exist between Sal and Try616, Gly586, Gly584, Thr587, and Lys583.

The CCK-8 assay was performed to determine the potential cytotoxic effects of Sal on chondrocytes. As shown in Fig. 3(B) and (C), Sal had a cell proliferative effect on human OA chondrocytes to various extents within the dose range of 5–100 μM, with the effect peaking at 40 μM. At the same time, dose-dependent pretreatment of Sal under these concentrations reversed TNF-α-induced cytotoxicity. In addition, as revealed by western blot analysis, both the increased expression of PCAF and acetylation of H3K9 in chondrocytes induced by TNF-α were inhibited by Sal pretreatment in a dose-dependent manner (Fig. 3(D) and (E)).

3.4. Pharmacological blockade of PCAF regulated the expression of extracellular matrix (ECM) proteins in human OA chondrocytes

To evaluate the degeneration of chondrocyte better, we detected the major ECM protein (collagen II and aggrecan) and ECM degrading enzymes (Mmp13 and Adamts5) of the chondrocyte by using ELISA and immunofluorescence. As shown in Fig. 4(A)–(D), TNF-α treatment significantly reduced collagen II and aggrecan expression, whereas it inhibited expression of Mmp13 and Adamts-5. However, all results from TNF-α were reversed by Sal
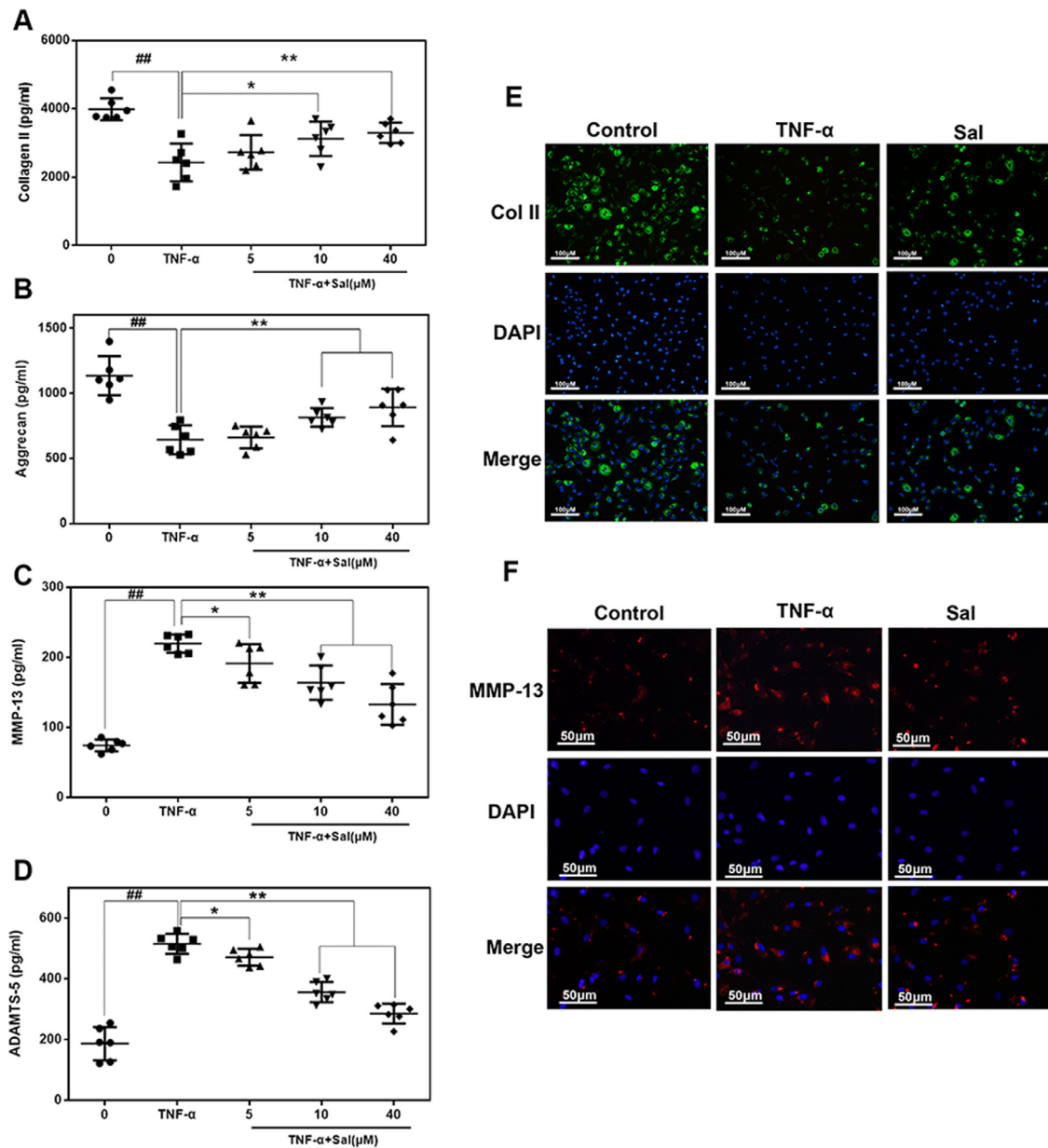
Fig. 4. Sal inhibited TNF-α-driven ECM degradation in human OA chondrocytes. (A–D) The levels of collagen II, aggrecan, MMP13, and ADAMTS-5 in the culture medium of chondrocytes treated as indicated. (E, F) Typical collagen-II and MMP13 were detected using immunofluorescence combined with DAPI staining of nuclei (scale bar: 100 μm [E], 50 μm [F]). All results are presented as the means ± SDs of six duplicate experiments. $^{\#\#}P < 0.01$ compared to the control group; $^{*}P < 0.05$, $^{**}P < 0.01$ compared to the TNF-α alone group.

in a dose-dependent manner (5, 10, and 40 μM). Additionally, immunofluorescence staining revealed that the expression of collagen II was higher, and that of MMP13 proteins was lower in the Sal-pretreated group, which was consistent with the ELISA results (Fig. 4(E) and (F)). Therefore, Sal exhibits a protective effect by regulating ECM expression under TNF-α treatment.

3.5. Pharmacological blockade of PCAF ameliorated TNF-α-induced inflammatory response and ER stress-related apoptosis in human chondrocytes

To examine the effect of Sal-mediated PCAF inhibition in the TNF-α-induced inflammatory response in human chondrocytes and explore the potential mechanism, we first assessed the expression of NO, PGE2, and IL-6 in TNF-α-treated human OA chondrocytes in the presence or absence of Sal. As shown in Fig. 5(A)–(C), the re-

sults indicated that TNF-α increased the production of NO, PGE2, and IL-6 significantly in chondrocytes compared to the control. Nevertheless, Sal dose-dependently inhibited TNF-α-induced NO, PGE2, and IL-6 expression. Next, we evaluated the effects of Sal on iNOS and COX-2 expression. Based on western blot results, Sal inhibited the up-regulation of TNF-α-induced protein expression of iNOS and COX-2 in a dose-dependent manner (Fig. 5(D) and (E)).

TNF-α-induced inflammation is mainly precipitated by the role of NF-κB. Mechanistically, the activation of NF-κB signaling was examined using western blotting and immunofluorescence. Western blot analysis revealed that TNF-α significantly stimulated IκBα degradation and caused the translocation of p65 into the nucleus; nevertheless, these effects induced by TNF-α were markedly restrained by Sal pretreatment in a dose-dependent manner (Fig. 5(F) and (G)). The immunofluorescence evaluation also revealed that p65 was translocated following NF-κB stimulation in TNF-α-
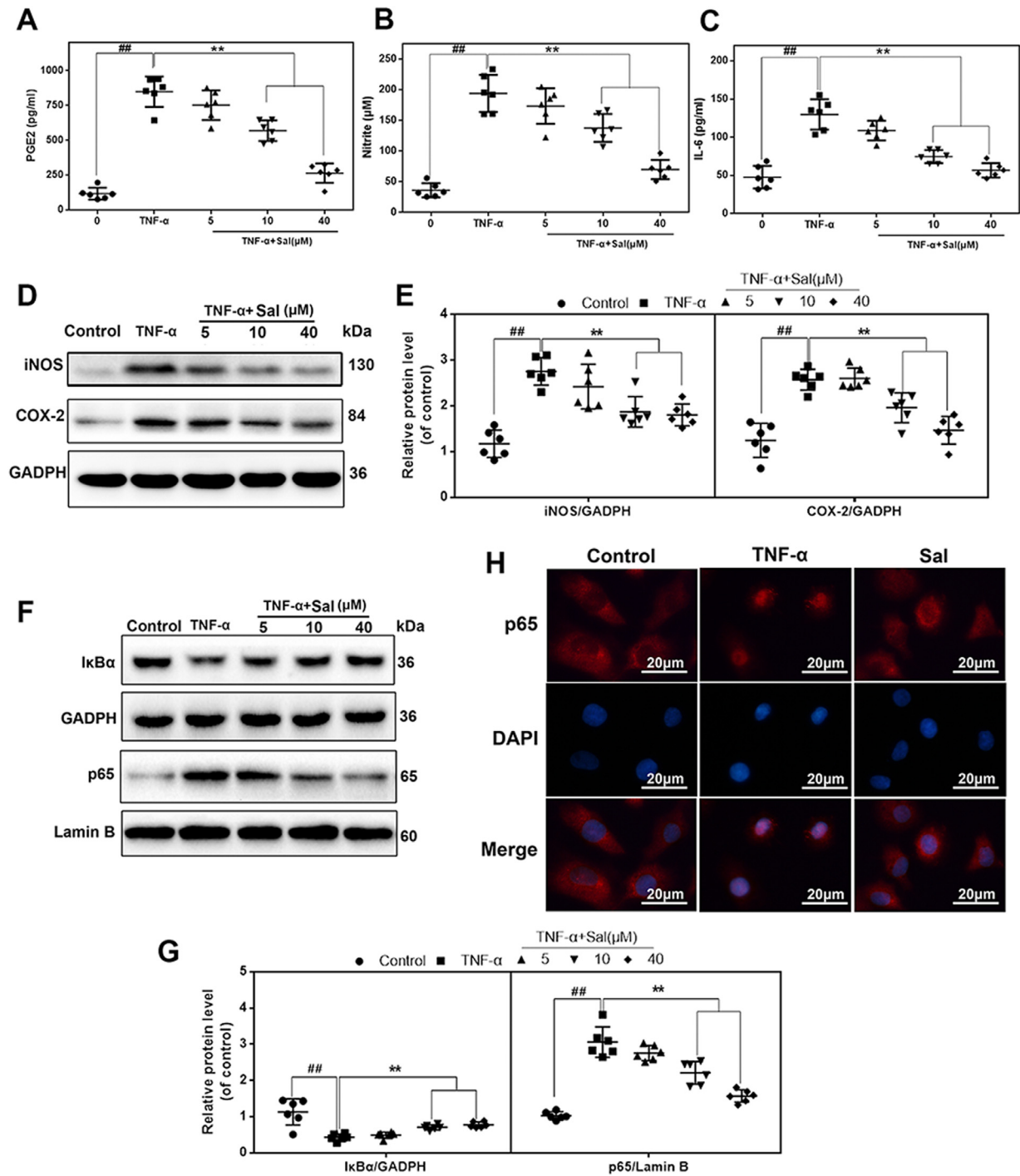
Fig. 5. Sal attenuated TNF-α-driven inflammation in human chondrocytes via inhibition of NF-κB signaling. (A–C) The levels of NO, PGE2, and IL-6 in the culture medium of human OA chondrocytes pretreated with Sal at different concentrations and stimulated with 20 ng/ml TNF-α. (D, E) The levels of iNOS and COX-2 in human chondrocytes pretreated with Sal at different concentrations and stimulated with 20 ng/ml TNF-α. (F, G) Cytoplasmic IκBα and nuclear p65 levels in human chondrocytes pretreated with Sal at different concentrations and stimulated with 20 ng/ml TNF-α. (H) The nuclear translocation of p65 was detected using immunofluorescence combined with DAPI staining of nuclei (scale bar: 20 μm). All results are presented as the means ± SDs of six duplicate experiments. $^{\#\#}P < 0.01$ compared to the control group; $^{*}P < 0.05$, $^{**}P < 0.01$ compared to the TNF-α alone group.

induced chondrocytes. The p65-active proteins were found mainly in the cytosol of the control group. Meanwhile, in the TNF-α-treated group, the p65-active proteins underwent dramatic movement from the cytosol to the nucleus. However, Sal alleviated the translocation of p65 (Fig. 5(H)).

To evaluate whether ER stress-related apoptosis is attenuated by Sal-induced PCAF inhibition, we investigated DNA damage using TUNEL staining and cleaved caspase 3 and PARP levels us-

ing western blotting. First, the apoptotic incidence detected using the TUNEL assay demonstrated that the apoptosis rates in Sal-treated nucleus pulposus cells were dramatically reduced (Fig. 6(A) and (B)). At the same time, western blot analysis revealed that Sal dose-dependently inhibited TNF-α-induced cleavage of caspase 3 and PARP (Fig. 6(C) and (D)). Second, a significant increase in ER stress-related proteins such as X-box binding protein 1S (XBP-1S), CHOP, cleaved caspase 12, and cytochrome C could also be
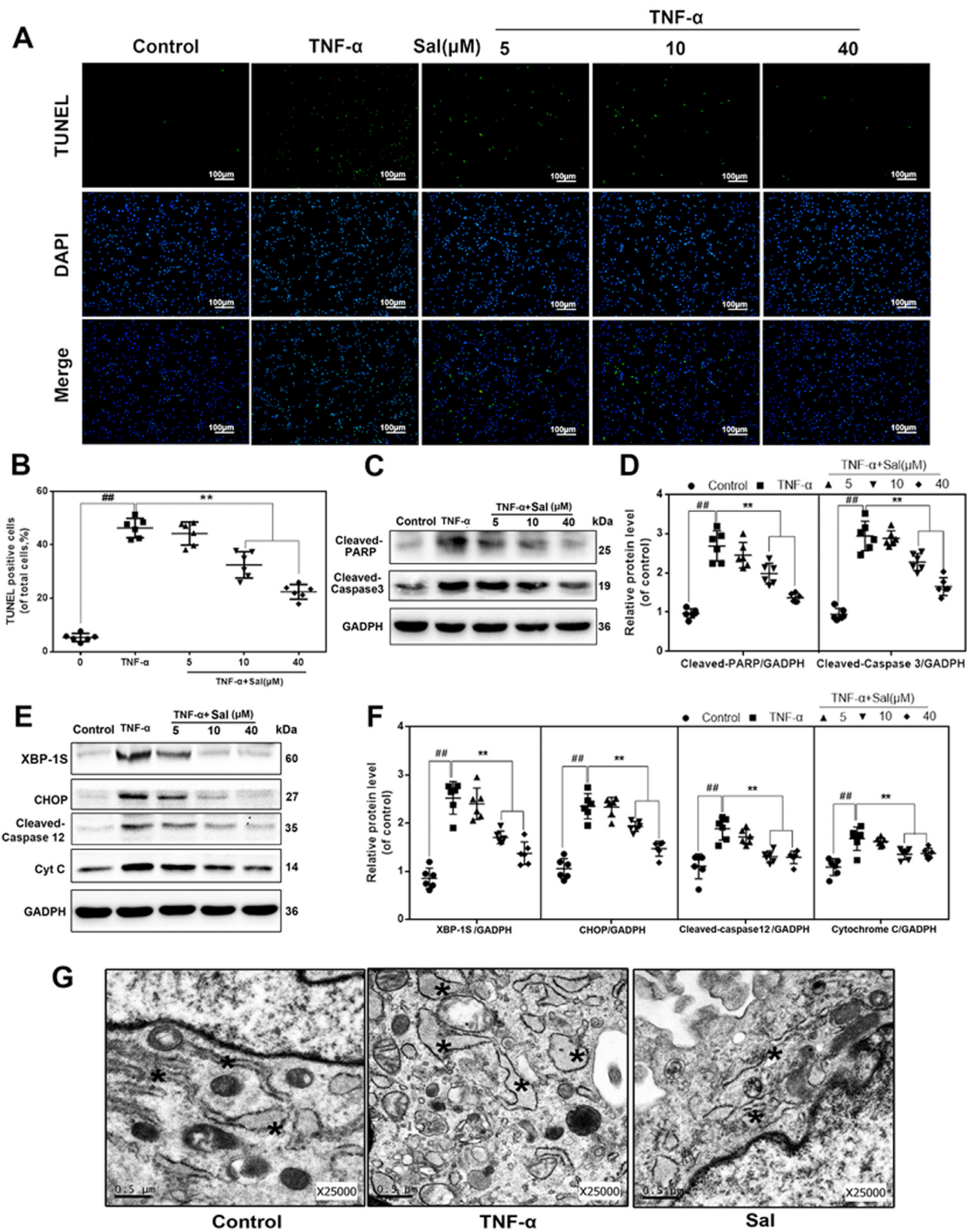
Fig. 6. Sal attenuated TNF-α-driven apoptosis in human chondrocytes via inhibition of ER stress. (A, B) TUNEL assay of apoptotic chondrocytes (scale bar: 100 μm). (C, D) The levels of cleaved caspase 3 and cleaved PARP in chondrocytes pretreated with Sal at different concentrations and stimulated with 20 ng/ml TNF-α. (E, F) The levels of XBP-1S, CHOP, cleaved caspase 12, and cytochrome C in chondrocytes pretreated with Sal at different concentrations and stimulated with 20 ng/ml TNF-α. (G) Electron microscopy images of chondrocytes exposed to stimulation with 20 ng/ml TNF-α with or without pretreatment with 40 μM Sal. All results are presented as the means ± SDs of six duplicate experiments. ##$P < 0.01$ compared to the control group; *$P < 0.05$, **$P < 0.01$ compared to the TNF-α alone group.
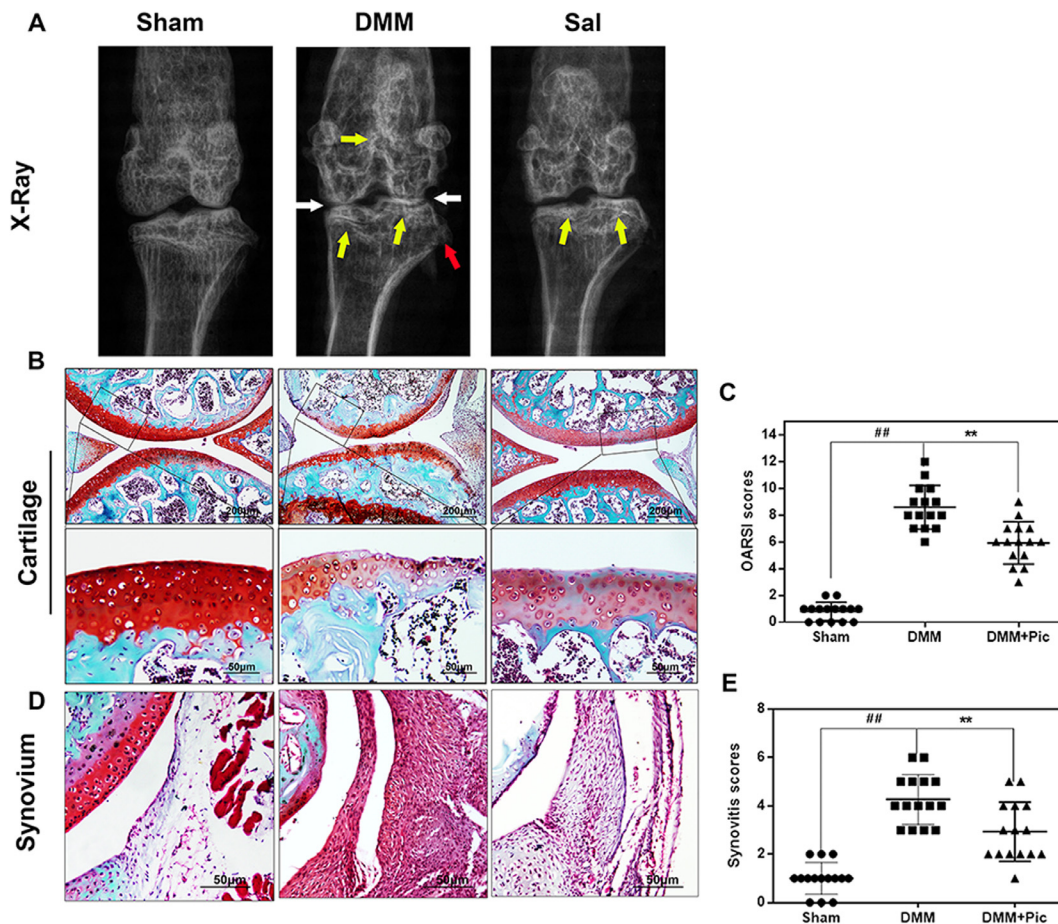
Fig. 7. Sal ameliorated OA development in an *in vivo* mouse DMM model. (A) Digital X-ray images of mouse knee joints from different experimental groups. The narrowing of joint space was observed in both the OA and treatment groups (white arrows), calcification of the cartilage surface was obvious in the DMM group (yellow arrows), and the red arrows indicate osteophyte formation. (B) Representative S-O staining of cartilage from different experimental groups at 8 weeks post-surgery (scale bar: 200 μm/50 μm). (C) The OARSI scores of cartilage sampled from the experimental groups. (D) Representative S–O staining of synovium from different experimental groups at 8 weeks post-surgery (scale bar: 50 μm). (E) The synovitis scores of cartilage sampled from the experimental groups. The data are presented as the means ± SDs ($n = 15$). Significant differences among groups are indicated as $^{\#\#}P < 0.01$ vs. the sham group; and $^{**}P < 0.01$ vs. the DMM group.

detected after TNF-α incubation, whereas Sal markedly inhibited this increase in a dose-dependent manner (Fig. 6(E) and (F)). In addition, the results of TEM showed similar changes. Compared to the control group, our results revealed that the ER in TNF-α-stimulated chondrocytes were more dilated and abundant. Meanwhile, these morphological changes were not observed in cells pretreated with Sal, confirming the results of the immunoblotting analysis (Fig. 6(G)).

3.6. Sal ameliorated OA development in mice in vivo

To determine the potential therapeutic effects of Sal on the induction and progression of OA *in vivo*, a surgically-induced DMM mouse model of OA was established. X-ray analysis revealed severe narrowing of joint space and greater calcification of cartilage surfaces in the DMM group than in the control. Nevertheless, these joint lesions (narrowing and calcification) were milder in the Sal-treated group (Fig. 7(A)). As revealed by S–O staining, the DMM mice exhibited superficial cartilage fibrillation, reduction of cartilage thickness, and massive proteoglycan loss, especially on the femur. Notably, the Sal-treated group exhibited richer proteoglycan content and less cartilage destruction compared to the DMM group (Fig. 7(B)). The OARSI score of the DMM group was obviously higher (8.60 ± 1.58) than that of the control (0.80 ± 0.65), whereas the Sal-treated group had markedly lower OARSI scores (5.93 ± 1.52) compared to the OA group (Fig. 7(C)). Synovial thick-

ening and hypercellularity were also observed in the OA group, whereas Sal treatment alleviated synovitis compared to the OA group (Control 1.00 ± 0.63 vs. DMM 4.27 ± 0.99 vs. DMM+Sal 2.93 ± 1.18; all $P < 0.01$; Fig. 6(D) and (E)). Taken together, these data suggest that Sal may play an important role in attenuating OA development.

3.7. Sal decreased PCAF expression, apoptosis, and inflammation in the mouse OA model

To investigate the underlying mechanism of the chondroprotective effects of Sal *in vivo*, we performed immunofluorescence staining of PCAF, TUNEL staining, and immunohistochemical staining of iNOS. The cartilage in the DMM group exhibited higher PCAF expression compared to the control group (Fig. 8(A) and (B)). Meanwhile, elevated iNOS (Fig. 7(E) and (F)) as well as TUNEL positive points (Fig. 8(C) and (D)) were also observed in the DMM group. Sal treatment significantly decreased the abundance of these stained proteins (Fig. 8).

4. Discussion

OA is a complex process of joint degeneration that is regulated by multiple factors, such as inflammatory mediators, mechanical forces, and transcriptional regulators [35]. Several epigenetic alterations, including the acetylation, methylation, ubiquitination, and
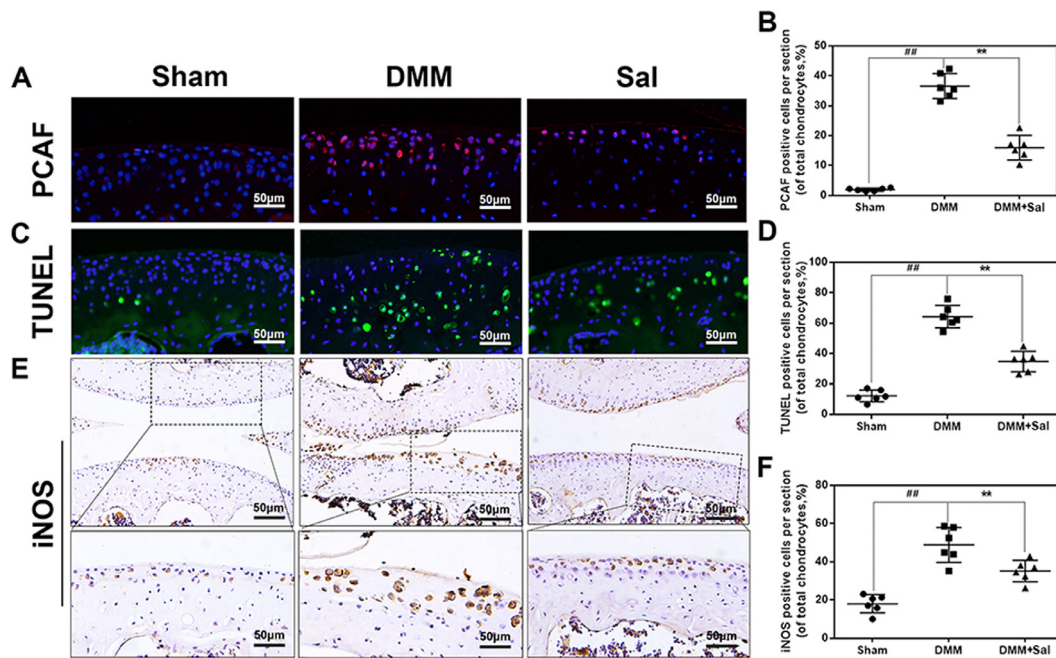
Fig. 8. Effects of Sal on PCAF expression, TUNEL staining, and iNOS expression in an *in vivo* mouse DMM model. (A, B) Immunofluorescence staining of PCAF expression in cartilage samples (scale bar: 50 μm). (C, D) TUNEL staining of cartilage samples (scale bar: 50 μm). (E, F) Immunohistochemical staining of iNOS expression in cartilage samples (scale bar: 50 μm). The data are presented as the means ± SDs ($n = 6$). Significant differences among different groups are indicated as $^{\#\#}P < 0.01$ vs. the sham group; and $^{**}P < 0.01$ vs. the DMM group.

phosphorylation of histone, have been shown to play important roles in the pathogenesis of OA [16,18,36,37]. Among them, the acetylation balance of histone mediated by HATs and HDACs is associated with the activation and inhibition of gene transcription in chondrocyte homeostasis [18]. For example, p300/CBP-induced histone acetylation leads to transcriptional activation of SOX9, a key regulator responsible for expression of the type II collagen gene (COL2A1) [38,39]. HDAC1 and HDAC2 were also reported to inhibit the expression of cartilage-specific genes in human chondrocytes [18]. Moreover, PCAF, as a member of the GCN5-related N-acetyltransferases targeting the acetylation of histone H3K9, was shown to be involved in the development of neurodegenerative disease [40–42]. However, its role in joint degenerative diseases such as OA is still unclear. In the present study, we found that the expression level of PCAF was significantly higher in OA cartilage and TNF-α-induced human chondrocytes, which subsequently promoted the acetylation of histone H3K9, indicating that aberrant acetylation mediated by PCAF contributes to the pathogenesis of OA.

IL-1β, IL-6, and TNF-α are the major proinflammatory cytokines in OA [15]. In particular, TNF-α is widely referred to as an effective stimulant, and enhanced production of NF-κB mediates an inflammatory response and ER stress-induced apoptosis in chondrocytes [7,11,12,15]. Both pathways play critical roles in OA development. In our present study, silencing PCAF not only dramatically decreased nuclear p65 levels but also inhibited CHOP (an ER stress marker) expression in TNF-α-stimulated chondrocytes. Therefore, the mechanism by which PCAF modulates OA may involve the inactivation of NF-κB and ER stress signals. This is in accord with previous studies carried out using a β-amyloid-mediated Alzheimer's disease model and high-glucose-stimulated pancreatic beta cells [23,42].

Currently, there are still few efficacious drugs for OA therapy, and side effects have made most drug candidates undesirable [43]. Thus, a variety of natural products have emerged as milder options for the treatment of OA in recent years [44,45]. Recent studies showed that salidroside (Sal) could protects against apoptosis

and inflammatory response in chondrocytes via inhibition of NF-κB activation and Phosphatidylinositol 3-Kinases (PI3K)/Akt Signaling [46–48]. However, the effect of Sal on osteoarthritis *in vivo* and the underlying mechanisms remains unclear. Numerous lines of evidence indicate that HATs may play positive roles as novel drug targets for the treatment of diseases related to inflammation and cell death [18,23,42]. The natural compound Sal is a starting point for the development of small-molecule inhibitors of histone acetylation [26]. To optimize its inhibitory potency on PCAF, a binding model for PCAF inhibition by Sal was proposed. The crystal structure of PCAF was downloaded from PDB which is in complex with coenzyme A (CoA) [49]. As previous study reported that the histone acetyltransferase activity of PCAF is stabilized by CoA as well as Acetyl-CoA, and the presence of CoA help to protects PCAF from proteolytic degradation [50]. Thus the binding site between CoA and PCAF was recognized as an inhibitory pockets for drug design since the structural stability would be decreased when the small molecule occupied this site. In our study, similarly, the inhibitory site of PCAF was the structural domain in which CoA bind with PCAF. This domain contains lots of amino acid residues such as Val582, Cys574, Try616, Gly584, Thr587 and Lys583, which were the main binding sites between salidroside and PCAF according to our results. The results indicated that Sal can directly occupy its inhibitory binding pocket, which was consistent with western blot results (Fig. 3(D)), suggesting that Sal is an effective inhibitor of PCAF. Additionally, our previous study demonstrated that Sal exerts anti-inflammatory and anti-apoptotic effects through the inhibition of NF-κB and ER stress cascades in LPS-stimulated microglia cells. Therefore, we further examined whether Sal-induced PCAF-inhibition could protect chondrocytes from TNF-α-mediated catabolism and whether the potential molecular mechanisms involved were related to the attenuation of inflammation and ER stress-associated apoptosis.

Multiple studies have found that PCAF is involved in the development of pancreatitis, arteriogenesis, and liver and renal injury, as PCAF plays an indispensable role in inflammation [51–53]. For example, the down-regulation of PCAF by miR-181a/b

provides negative feedback regulation to TNF-α-induced inflammatory reaction in liver epithelial cells [53]. Meanwhile, it is well recognized that p300/CBP and PCAF are transcriptional coactivators of NF-κB signaling. PCAF mediated acetylation of Lys-122 residue of NF-κB and the NF-κB pathway is of vital importance in the development of OA as it elicits inflammation that causes matrix degradation [19,54]. NF-κB signaling participates in the production of inflammatory mediators, including NO and PGE2, which are both core inflammatory mediators in the pathogenesis of OA and are generated by iNOS and COX-2, respectively [55,56]. These mediators contribute to MMP and ADAMTS secretion, leading to the degradation of the ECM [57]. In this study, we demonstrated that the salidroside occupied the inhibitory pockets and the acetylating ability and expression level of PCAF would be decreased due to the loss of structural stability. Meanwhile pharmacological inhibition of PCAF by Sal can specifically inhibit inflammatory mediator secretion via interaction with the NF-κB pathway.

In addition to its positive role in anti-inflammatory effects, PCAF also participates in the regulation of cell growth, ER stress, and mitosis [58]. It has been shown that PCAF binds to XBP-1S, an important regulator inducing ER stress cascade processes, including cellular unfolded protein response, integrated stress response, and ER-associated death [23]. ER stress has been well-recognized as one of the most significant factors in the process of OA pathogenesis [59]. Moderate ER stress is an adaptive protective process in chondrocytes, but malfunction in the ER resulting from excessive ER stress can lead to cellular dysfunction. Excessive ER stress initiates the cleavage of caspase 12 and finally induces cell apoptosis [13]. CHOP acts as a canonical marker of ER stress [59]. In our study, pharmacological inhibition of PCAF by Sal significantly reduced the levels of CHOP and cleaved caspase, indicating that Sal-mediated PCAF inhibition attenuates TNF-α-induced ER stress. In addition, aberrant ER stress leads to the activation of a series of caspases and PARP, followed by further DNA damage. Our results demonstrated that Sal administration markedly decreased chondrocytes apoptosis and levels of cleaved caspase 3 and cleaved PARP, which were up-regulated by TNF-α treatment. These results indicate that pharmacological inhibition of PCAF by Sal ameliorates apoptosis in chondrocytes by stabilizing excessive ER stress.

OA progression involves the loss of proteoglycans on the cartilage surface, calcification changes, chondrocyte apoptosis, and synovitis [1,44]. To characterize the specific functions of Sal-mediated PCAF inhibition in OA *in vivo*, a DMM mouse model was established. We found that Sal significantly reduced OARSI scores, subchondral thickness, and severity scores of synovitis in DMM mice. In addition, the Sal-reduced apoptosis and decreased levels of iNOS were consistent with the inhibition of PCAF expression, indicating that this a potential mechanism underlying the pharmacological inhibition of PCAF by Sal *in vivo*.

Our study has some limitations. Firstly, studies showed that chondrocytes undergo a process of dedifferentiation in monolayer culture that is characterized by a transition to a fibroblast-like phenotype [60]. Thus in order to prevent phenotypic feature loss, passage 1–3 chondrocytes were used in our most studies.3D culture may offer a possible way to the maintenance of cartilaginous gene expression on extracellular matrix [61], which would be applied for our further study. Secondly, Destabilization of medial meniscus (DMM) model is used in our study, which is also the most commonly used surgical model for OA in mice currently. However, the mice used are always young and postsurgical healing responses and inability to rigorously control the mechanical loading environment within the affected joint may complicate the situation [62]. As OA is a multifactorial disease, different models (mechanical loading models; spontaneous and genetic models; high-fat dietary and/or obesity models) have their respective advantages in exploring individual aspects of the disease, more models could be used in our further study.

In summary, our findings demonstrate that PCAF is an essential regulator for chondrocyte homeostasis and OA development, and specifically, the inhibition of PCAF expression via Sal administration may provide a promising therapeutic strategy for OA treatment.

Declaration of Competing Interest

The authors declare no conflict of interests.

CRediT authorship contribution statement

Deheng Chen: Writing - review & editing. **Di Lu:** Data curation, Writing - review & editing. **Haixiao Liu:** Investigation, Data curation. **Enxing Xue:** Investigation, Data curation. **Yu Zhang:** Supervision. **Ping Shang:** Data curation, Writing - review & editing. **Xiaoyun Pan:** Formal analysis, Writing - review & editing.

Acknowledgments

Funding source

References

[1] Glyn-Jones S, Palmer AJ, Agricola R, Price AJ, Vincent TL, Weinans H, et al. Osteoarthritis. Lancet 2015;386(9991):376–87.

[2] Blagojevic M, Jinks C, Jeffery A, Jordan KP. Risk factors for onset of osteoarthritis of the knee in older adults: a systematic review and meta-analysis. Osteoarthr Cartil 2010;18(1):24–33.

[3] Loeser RF. Aging and osteoarthritis: the role of chondrocyte senescence and aging changes in the cartilage matrix. Osteoarthr Cartil 2009;17(8):971–9.

[4] Kapoor M, Martel-Pelletier J, Lajeunesse D, Pelletier JP, Fahmi H. Role of proinflammatory cytokines in the pathophysiology of osteoarthritis. Nat Rev Rheumatol 2011;7(1):33–42.

[5] Bay-Jensen AC, Henrotin Y, Karsdal M, Mobasheri A. The need for predictive, prognostic, objective and complementary blood-based biomarkers in osteoarthritis (OA). EBioMedicine 2016;7:4–6.

[6] Liacini A, Sylvester J, Li WQ, Huang W, Dehnade F, Ahmad M, et al. Induction of matrix metalloproteinase-13 gene expression by TNF-alpha is mediated by MAP kinases, AP-1, and NF-kappaB transcription factors in articular chondrocytes. Exp Cell Res 2003;288(1):208–17.

[7] Guo FJ, Xiong Z, Lu X, Ye M, Han X, Jiang R. ATF6 upregulates XBP1S and inhibits ER stress-mediated apoptosis in osteoarthritis cartilage. Cell Signal 2014;26(2):332–42.

[8] Smith MD, Triantafillou S, Parker A, Youssef PP, Coleman M. Synovial membrane inflammation and cytokine production in patients with early osteoarthritis. J Rheumatol 1997;24(2):365–71.

[9] Hulejova H, Baresova V, Klezl Z, Polanska M, Adam M, Senolt L. Increased level of cytokines and matrix metalloproteinases in osteoarthritic subchondral bone. Cytokine 2007;38(3):151–6.

[10] Nah SS, Choi IY, Yoo B, Kim YG, Moon HB, Lee CK. Advanced glycation end products increases matrix metalloproteinase-1, -3, and -13, and TNF-alpha in human osteoarthritic chondrocytes. FEBS Lett 2007;581(9):1928–32.

[11] Tak PP, Firestein GS. NF-kappaB: a key role in inflammatory diseases. J Clin Invest 2001;107(1):7–11.

[12] Lopez-Armada MJ, Carames B, Lires-Dean M, Cillero-Pastor B, Ruiz-Romero C, Galdo F, et al. Cytokines, tumor necrosis factor-alpha and interleukin-1beta, differentially regulate apoptosis in osteoarthritis cultured human chondrocytes. Osteoarthr Cartil 2006;14(7):660–9.

[13] Schroder M, Kaufman RJ. ER stress and the unfolded protein response. Mutat Res 2005;569(1–2):29–63.

[14] Shu S, Zhu J, Liu Z, Tang C, Cai J, Dong Z. Endoplasmic reticulum stress is activated in post-ischemic kidneys to promote chronic kidney disease. EBioMedicine 2018;37:269–80.

[15] Liu-Bryan R, Terkeltaub R. Emerging regulators of the inflammatory process in osteoarthritis. Nat Rev Rheumatol 2015;11(1):35–44.

[16] Kim H, Kang D, Cho Y, Kim JH. Epigenetic regulation of chondrocyte catabolism and anabolism in osteoarthritis. Mol Cells 2015;38(8):677–84.

[17] Raman S, FitzGerald U, Murphy JM. Interplay of inflammatory mediators with epigenetics and cartilage modifications in osteoarthritis. Front Bioeng Biotechnol 2018;6:22.

[18] Khan NM, Haqqi TM. Epigenetics in osteoarthritis: potential of HDAC inhibitors as therapeutics. Pharmacol Res 2018;128:73–9.

[19] Ghizzoni M, Boltjes A, Graaf C, Haisma HJ, Dekker FJ. Improved inhibition of the histone acetyltransferase PCAF by an anacardic acid derivative. Bioorg Med Chem 2010;18(16):5826–34.

[20] Zheng X, Gai X, Ding F, Lu Z, Tu K, Yao Y, et al. Histone acetyltransferase PCAF up-regulated cell apoptosis in hepatocellular carcinoma via acetylating histone H4 and inactivating AKT signaling. Mol Cancer 2013;12(1):96.

[21] Sun C, Wang M, Liu X, Luo L, Li K, Zhang S, et al. PCAF improves glucose homeostasis by suppressing the gluconeogenic activity of PGC-1alpha. Cell Rep 2014;9(6):2250–62.

[22] Ghizzoni M, Haisma HJ, Maarsingh H, Dekker FJ. Histone acetyltransferases are crucial regulators in NF-kappaB mediated inflammation. Drug Discov Today 2011;16(11–12):504–11.

[23] Rabhi N, Denechaud PD, Gromada X, Hannou SA, Zhang H, Rashid T, et al. KAT2B is required for pancreatic beta cell adaptation to metabolic stress by controlling the unfolded protein response. Cell Rep 2016;15(5):1051–61.

[24] Dekker FJ, Ghizzoni M, van der Meer N, Wisastra R, Haisma HJ. Inhibition of the PCAF histone acetyl transferase and cell proliferation by isothiazolones. Bioorg Med Chem 2009;17(2):460–6.

[25] Stimson L, Rowlands MG, Newbatt YM, Smith NF, Raynaud FI, Rogers P, et al. Isothiazolones as inhibitors of PCAF and p300 histone acetyltransferase activity. Mol Cancer Ther 2005;4(10):1521–32.

[26] Qi Z, Zhang Y, Qi S, Ling L, Gui L, Yan L, et al. Salidroside inhibits HMGB1 acetylation and release through upregulation of SirT1 during inflammation. Oxid Med Cell Longev 2017;2017:1–11.

[27] Wang C, Lou Y, Xu J, Feng Z, Chen Y, Tang Q, et al. Endoplasmic reticulum stress and NF-[Formula: see text]B pathway in salidroside mediated neuroprotection: potential of salidroside in neurodegenerative diseases. Am J Chin Med 2017;45(7):1459–75.

[28] World Medical A. World medical association declaration of Helsinki: ethical principles for medical research involving human subjects. JAMA 2013;310(20):2191–4.

[29] Au RY, Al-Talib TK, Au AY, Phan PV, Frondoza CG. Avocado soybean unsaponifiables (ASU) suppress TNF-alpha, IL-1beta, COX-2, iNOS gene expression, and prostaglandin E2 and nitric oxide production in articular chondrocytes and monocyte/macrophages. Osteoarthr Cartil 2007;15(11):1249–55.

[30] Glasson SS, Blanchet TJ, Morris EA. The surgical destabilization of the medial meniscus (DMM) model of osteoarthritis in the 129/SvEv mouse. Osteoarthr Cartil 2007;15(9):1061–9.

[31] Deheng C, Kailiang Z, Weidong W, Haiming J, Daoliang X, Ningyu C, et al. Salidroside promotes random skin flap survival in rats by enhancing angiogenesis and inhibiting apoptosis. J Reconstr Microsurg 2016;32(8):580–586.

[32] Glasson SS, Chambers MG, Van Den Berg WB, Little CB. The OARSI histopathology initiative – recommendations for histological assessments of osteoarthritis in the mouse. Osteoarthr Cartil 2010;18(Suppl 3):S17–23.

[33] Lewis JS, Hembree WC, Furman BD, Tippets L, Cattel D, Huebner JL, et al. Acute joint pathology and synovial inflammation is associated with increased intra-articular fracture severity in the mouse knee. Osteoarthr Cartil 2011;19(7):864–73.

[34] Shi S, Lin J, Cai Y, Yu J, Hong H, Ji K, et al. Dimeric structure of p300/CBP associated factor. BMC Struct Biol 2014;14:2.

[35] Loeser RF. Molecular mechanisms of cartilage destruction: mechanics, inflammatory mediators, and aging collide. Arthritis Rheum 2006;54(5):1357–60.

[36] Ramos YF, Meulenbelt I. The role of epigenetics in osteoarthritis: current perspective. Curr Opin Rheumatol 2017;29(1):119–29.

[37] Zheng C, Lin X, Xu X, Wang C, Zhou J, Gao B, et al. Suppressing UPR-dependent overactivation of FGFR3 signaling ameliorates SLC26A2-deficient chondrodysplasias. EBioMedicine 2019;40:695–709.

[38] DeLise AM, Fischer L, Tuan RS. Cellular interactions and signaling in cartilage development. Osteoarthr Cartil 2000;8(5):309–34.

[39] Furumatsu T, Asahara H. Histone acetylation influences the activity of Sox9-related transcriptional complex. Acta Med Okayama 2010;64(6):351–7.

[40] Bodai L, Pallos J, Thompson LM, Marsh JL. Pcaf modulates polyglutamine pathology in a Drosophila model of Huntington's disease. Neurodegener Dis 2012;9(2):104–6.

[41] Jin Q, Yu LR, Wang L, Zhang Z, Kasper LH, Lee JE, et al. Distinct roles of GCN5/PCAF-mediated H3K9ac and CBP/p300-mediated H3K18/27ac in nuclear receptor transactivation. EMBO J 2011;30(2):249–62.

[42] Park SY, Kim MJ, Kim YJ, Lee YH, Bae D, Kim S, et al. Selective PCAF inhibitor ameliorates cognitive and behavioral deficits by suppressing NF-kappaB-mediated neuroinflammation induced by Abeta in a model of Alzheimer's disease. Int J Mol Med 2015;35(4):1109–18.

[43] Smith SR, Deshpande BR, Collins JE, Katz JN, Losina E. Comparative pain reduction of oral non-steroidal anti-inflammatory drugs and opioids for knee osteoarthritis: systematic analytic review. Osteoarthr Cartil 2016;24(6):962–72.

[44] Tang Q, Zheng G, Feng Z, Chen Y, Lou Y, Wang C, et al. Trehalose ameliorates oxidative stress-mediated mitochondrial dysfunction and ER stress via selective autophagy stimulation and autophagic flux restoration in osteoarthritis development. Cell Death Dis 2017;8(10):e3081.

[45] Tang Q, Feng Z, Tong M, Xu J, Zheng G, Shen L, et al. Piceatannol inhibits the IL-1beta-induced inflammatory response in human osteoarthritic chondrocytes and ameliorates osteoarthritis in mice by activating Nrf2. Food Funct 2017;8(11):3926–37.

[46] Zhang Y, Zhao Q. Salidroside attenuates interleukin-1beta-induced inflammation in human osteoarthritis chondrocytes. J Cell Biochem 2018:1–7.

[47] Wu M, Hu R, Wang J, An Y, Lu L, Long C, et al. Salidroside suppresses IL-1beta-induced apoptosis in chondrocytes via phosphatidylinositol 3-Kinases (PI3K)/Akt signaling inhibition. Med Sci Monit: Int Med J Exp Clin Res 2019;25:5833–40.

[48] Liu M, Zhang J, Liu W, Wang W. Salidroside protects ATDC5 cells against lipopolysaccharide-induced injury through up-regulation of microRNA-145 in osteoarthritis. Int Immunopharmacol 2019;67:441–8.

[49] Shi S, Lin J, Cai Y, Yu J, Hong H, Ji K, et al. Dimeric structure of p300/CBP associated factor. BMC Struct Biol 2014;14:2 undefined.

[50] Herrera JE, Bergel M, Yang XJ, Nakatani Y, Bustin M. The histone acetyltransferase activity of human GCN5 and PCAF is stabilized by coenzymes. J Biol Chem 1997;272(43):27253–8.

[51] Bastiaansen AJ, Ewing MM, de Boer HC, van der Pouw Kraan TC, de Vries MR, Peters EA, et al. Lysine acetyltransferase PCAF is a key regulator of arteriogenesis. Arterioscler Thromb Vasc Biol 2013;33(8):1902–10.

[52] Sandoval J, Pereda J, Rodriguez JL, Escobar J, Hidalgo J, Joosten LA, et al. Ordered transcription factor recruitment and epigenetic regulation of tnf-alpha in necrotizing acute pancreatitis. Cell Mol Life Sci 2010;67(10):1687–97.

[53] Zhao J, Gong AY, Zhou R, Liu J, Eischeid AN, Chen XM. Downregulation of PCAF by miR-181a/b provides feedback regulation to TNF-alpha-induced transcription of proinflammatory genes in liver epithelial cells. J Immunol 2012;188(3):1266–74.

[54] Rigoglou S, Papavassiliou AG. The NF-kappaB signalling pathway in osteoarthritis. Int J Biochem Cell Biol 2013;45(11):2580–4.

[55] Sasaki K, Hattori T, Fujisawa T, Takahashi K, Inoue H, Takigawa M. Nitric oxide mediates interleukin-1-induced gene expression of matrix metalloproteinases and basic fibroblast growth factor in cultured rabbit articular chondrocytes. J Biochem 1998;123(3):431–9.

[56] Hardy MM, Seibert K, Manning PT, Currie MG, Woerner BM, Edwards D, et al. Cyclooxygenase 2-dependent prostaglandin E2 modulates cartilage proteoglycan degradation in human osteoarthritis explants. Arthritis Rheum 2002;46(7):1789–803.

[57] Tang Q, Zheng G, Feng Z, Tong M, Xu J, Hu Z, et al. Wogonoside inhibits IL-1beta induced catabolism and hypertrophy in mouse chondrocyte and ameliorates murine osteoarthritis. Oncotarget 2017;8(37):61440–56.

[58] Huang J, Wan D, Li J, Chen H, Huang K, Zheng L. Histone acetyltransferase PCAF regulates inflammatory molecules in the development of renal injury. Epigenetics 2015;10(1):62–71.

[59] Uehara Y, Hirose J, Yamabe S, Okamoto N, Okada T, Oyadomari S, et al. Endoplasmic reticulum stress-induced apoptosis contributes to articular cartilage degeneration via C/EBP homologous protein. Osteoarthr Cartil 2014;22(7):1007–17.

[60] Hoshiba T, Yamada T, Lu H, Kawazoe N, Chen G. Maintenance of cartilaginous gene expression on extracellular matrix derived from serially passaged chondrocytes during in vitro chondrocyte expansion. J Biomed Mater Res Part A 2012;100(3):694–702.

[61] Grogan SP, Duffy SF, Pauli C, Latz MK, D'Lima DD. Gene expression profiles of the meniscus avascular phenotype: a guide for meniscus tissue engineering. J Orthop Res: Off Publ Orthop Res Soc 2018;36(7):1947–58.

[62] Fang H, Beier F. Mouse models of osteoarthritis: modelling risk factors and assessing outcomes. Nat Rev Rheumatol 2014;10(7):413–21.